JMEPEG (2016) 25:1150–1156
DOI: 10.1007/s11665-016-1914-x

1059-9495/$19.00

Hot Deformation and Dynamic Recrystallization Behavior of the Cu-Cr-Zr-Y Alloy

Yi Zhang, Sun Huili, Alex A. Volinsky, Baohong Tian, Zhe Chai, Ping Liu, and Yong Liu

(Submitted November 25, 2015; in revised form January 9, 2016; published online January 25, 2016)

To study the workability and to optimize the hot deformation processing parameters of the Cu-Cr-Zr-Y alloy, the strain hardening effect and dynamic softening behavior of the Cu-Cr-Zr-Y alloy were investigated. The flow stress increases with the strain rate and stress decreases with deformation temperature. The critical conditions, including the critical strain and stress for the occurrence of dynamic recrystallization, were determined based on the alloy strain hardening rate. The critical stress related to the onset of dynamic recrystallization decreases with temperature. The evolution of DRX microstructure strongly depends on the deformation temperature and the strain rate. Dynamic recrystallization appears at high temperatures and low strain rates. The addition of Y can refine the grain and effectively accelerate dynamic recrystallization. Dislocation generation and multiplication are the main hot deformation mechanisms for the alloy. The deformation temperature increase and the strain rate decrease can promote dynamic recrystallization of the alloy.

Keywords Cu-Cr-Zr-Y alloy, dynamic recrystallization, hot deformation, metals and alloys, microstructure

1. Introduction

Cu-Cr-Zr alloys have been widely used for many applications, such as railway contact wires, electrodes for resistance welding, and integrated circuit lead-frame materials, due to their high strength, outstanding electrical properties, thermal conductivity, and excellent fatigue resistance. Multiple studies have been carried out on the Cu-Cr-Zr alloys, and most of them focused on improving physical and mechanical properties, such as ductility, thermal stability, fatigue resistance, recrystallization behavior after cold rolling, strength, and conductivity [1–3]. The dynamic recovery (DRV) and dynamic recrystallization (DRX) occurring during the hot deformation processing are important for obtaining suitable microstructure, which can influence mechanical and functional properties of the material and hence its applicability. There are some investigations of hot deformation of the Cu-Cr-Zr alloys. Ding et al. [4] studied the Cu-0.6Cr-0.03Zr alloy and found that the dynamic recrystallization developed completely at 750 and 850 °C when the grain dimensions increase with decreasing strain rate and increasing deformation temperature. Ji et al. [5] found that under the test conditions the deformation activation energy of the Cu-0.36Cr-0.03Zr alloy was 432.6 KJ/mol, and an experimentally based constitutive model was developed to predict the flow stress of the alloy during high temperature deformation. Zhang et al. [6] found that the addition of Ce can improve the Cu-Cr-Zr alloy deformation activation energy during hot deformation. However, relations between the important points of the flow curves and the critical conditions for DRX initiation during hot working require further investigation.

In this paper, the effects of deformation parameters, including temperature and strain rate, on the flow stress of the Cu-Cr-Zr-Y alloy have been investigated by hot compression tests. The critical conditions for DRX of the alloy were determined by changing the strain rate. The microstructure evolution of this alloy was characterized under different hot deformation conditions. The results and the related discussion help optimize hot deformation processing parameters of the Cu-Cr-Zr-Y alloy.

2. Experimental Details

The Cu-Cr-Zr-Y alloy was prepared using pure Cu, Cr, Zr, and Y by melting in a vacuum induction furnace in argon, and then cast into a low carbon steel mold with Φ 83 mm × 150 mm dimensions. The chemical composition in wt.% of this alloy is: 0.4 Cr, 0.15 Zr, 0.04 Y, and Cu balance. The ingot was homogenized at 930 °C for 2 h to remove the alloying element segregation. Subsequently, the ingot was forged into 25 mm diameter bars. Finally, the forged bars were solution treated at 900 °C for 1 h, followed by water quenching.

Cylindrical compression specimens with 8 mm diameter and 12 mm high were machined from the solution-treated bars. Hot compression tests were carried out using the Gleeble-1500D thermomechanical simulator at a strain rate of 0.001-10 s^{-1} and

Yi Zhang, School of Materials Science and Engineering, Henan University of Science and Technology, Luoyang 471003, China; Department of Mechanical Engineering, University of South Florida, Tampa 33620; and Collaborative Innovation Center of Nonferrous Metals, Luoyang 471003 Henan, China; **Sun Huili, Baohong Tian,** and **Yong Liu**, School of Materials Science and Engineering, Henan University of Science and Technology, Luoyang 471003, China and Collaborative Innovation Center of Nonferrous Metals, Luoyang 471003 Henan, China; **Alex A. Volinsky**, Department of Mechanical Engineering, University of South Florida, Tampa 33620; **Zhe Chai**, School of Materials Science and Engineering, Henan University of Science and Technology, Luoyang 471003, China; and **Ping Liu**, School of Materials Science and Engineering, University of Shanghai for Science and Technology, Shanghai 200093, China. Contact e-mails: zhshgu436@163.com, volinsky@eng.usf.edu, and volinsky@usf.edu.

deformation temperature of 650-850 °C. The specimens were heated to the deformation temperature at 5 °C/s heating rate. Before deformation all specimens were kept at the deformation temperature for 180 s. All specimens were compressed to a true strain of 0.6. After compression testing, the specimens were immediately quenched in water. The deformed specimens were sectioned parallel to the compression axis. All specimens were polished and then etched with a solution of $FeCl_3$ (5 g) + C_2H_5OH (85 mL) + HCl (10 mL). Transmission electron microscopy (TEM) samples were prepared using Gatan 691 ion beam thinner. The precipitated phase was characterized using JEM-2100 (Jeol, Japan) high-resolution transmission electron microscope (HRTEM).

3. Results and Discussion

3.1 Flow Stress Behavior

The true stress-true strain curves obtained for the Cu-Cr-Zr-Y alloy at various strain rates and deformation temperatures are shown in Fig. 1. The flow stress increases with the strain rate and stress decreases with the deformation temperature. Thus, the deformation strain rate and temperature have great effects on the alloy during hot deformation process. The flow stress rapidly increases to a peak value, and then gradually decreases to a relatively steady value at higher temperatures and lower strain rates. Typical dynamic recrystallization (DRX) behavior was observed at the deformation temperatures of 750, 800, and 850 °C, respectively in Fig. 1(a). Similar results were obtained at 850 °C deformation temperature in Fig. 1(b). It is well known that the hot deformation is a competition process between the strain hardening and the dynamic softening [7]. During the initial hot deformation stage it is due to the rapid multiplication of dislocations leading to the strain hardening exceeding dynamic softening. After this the flow stress increases rapidly. With the increasing strain, the dynamic recovery and dynamic recrystallization play dominant roles. The flow stress increases accompanied by a decreasing hardening rate at higher strain, until the peak stress is reached. When the dynamic softening rate is higher than the strain hardening rate, the stress gradually reduces until a new balance between the softening and the hardening is achieved.

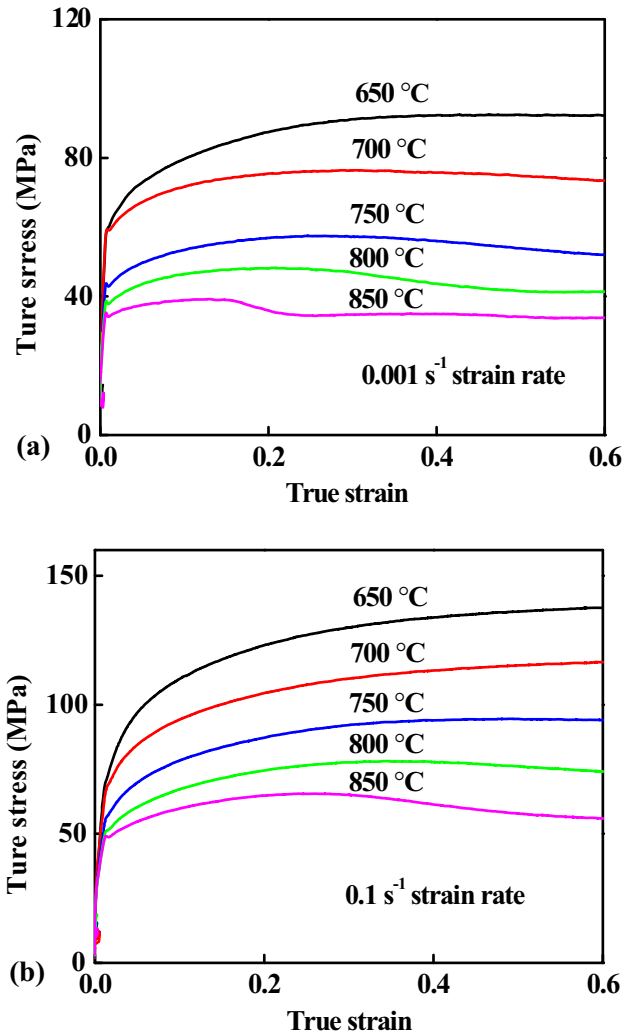

Fig. 1 True stress-strain curves of the Cu-Cr-Zr-Y alloy under different deformation conditions

It can be seen that continuous strain hardening was observed at the deformation temperature of 650 °C in Fig. 1. The main reason for such phenomenon is lack of time for energy accumulation and lower grain boundaries mobility at higher strain rate or lower temperature. The reduction of deformation time restrains the growth of DRX grains and increases the strain hardening effect [8].

3.2 Strain Hardening Behavior

The critical strain ε_c of the material in Fig. 2(a) determines the DRX onset. This is an effective method to determine the critical strain based on the flow stress curves. The strain hardening rate θ ($d\sigma/d\varepsilon$) derived from the true stress-strain curve is one of the most important factors for hot deformation evaluation [9]. The effects of temperature, strain rate, and strain on the strain hardening rate θ ($d\sigma/d\varepsilon$) are shown in Fig. 2. The strain hardening rate has a sharp drop until reaching a plateau. A negative value of the strain hardening rate was observed in Fig. 2, except for the 650 °C. The strain hardening values of the alloy deformed at 650 °C are much higher than the other specimens deformed at higher temperatures. A negative value of the strain hardening rate is associated with the flow softening due to the occurrence of DRX [10]. Thus, DRX did not occur at the 650 °C deformation temperature. The inflection point is marked by an arrow in Fig. 2(a) and is clear for the critical strain ε_c of the alloy deformed at 850 °C with the strain rate of 0.001 s^{-1}. A minimum value of θ was observed in Fig. 2(a) at 850 °C and reflects the maximum softening rate at ε_s.

3.3 Critical Conditions for DRX

It is generally considered that DRX begins at the peak stress of the flow stress-strain curves. However, in this case DRX starts at the critical stress before the peak stress occurs [11]. In previous research, several mathematical models were established to predict the critical conditions for DRX, i.e., the dislocation hardening model [12], nucleation mechanism of static recrystallization model [13], and so on. Najafizadeh et al. [14] fitted the third-order polynomial to the θ-σ curves to determine the critical conditions for DRX. This method was applied in this study as well. In this model, the maximum local stored energy and the minimum dissipation rate values must be satisfied for the onset of dynamic recrystallization. The corresponding location for the DRX onset in the flow curves is defined by the inflection point of the strain hardening rate vs. stress (θ-σ) plot. The associated

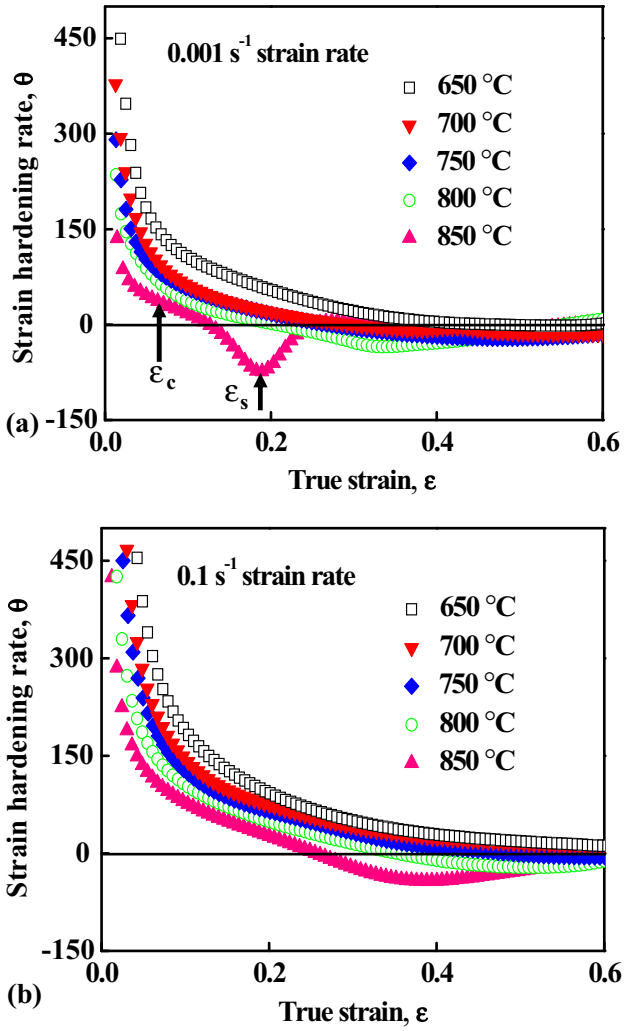

Fig. 2 Strain hardening rate variation of the Cu-Cr-Zr-Y alloy under different deformation temperature at the true strain of: (a) 0.001 s^{-1} and (b) 0.1 s^{-1}

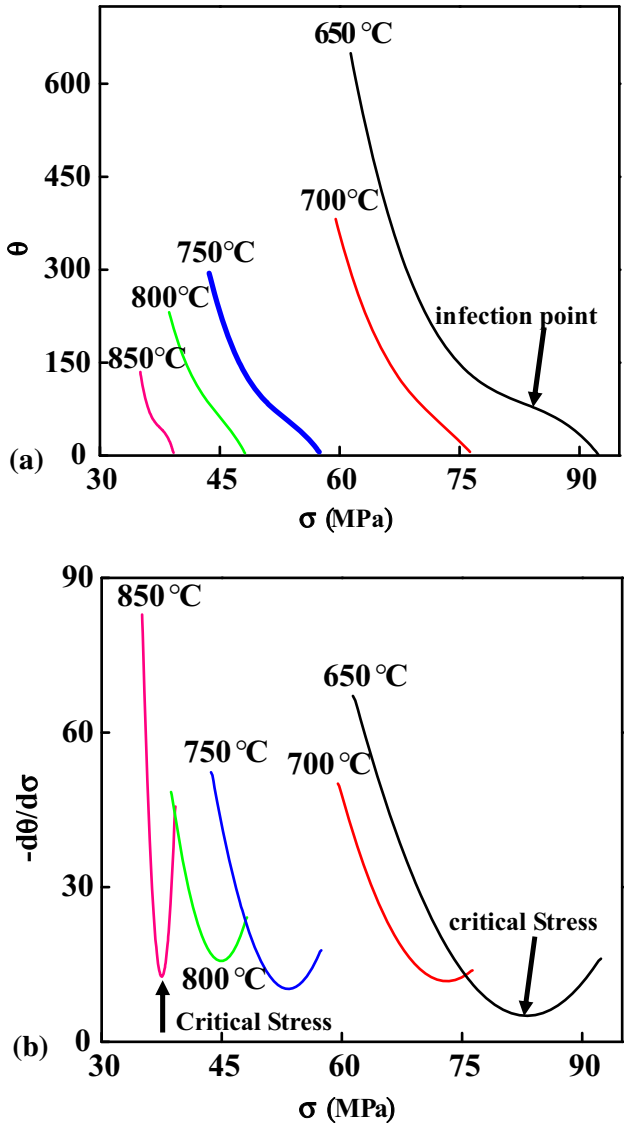

Fig. 3 (a) Strain hardening rate θ as a function of the true stress σ; (b) the true stress σ dependence of $-d\theta/d\sigma$ for the Cu-Cr-Zr-Y alloy at different temperatures under the strain rate of 0.001 s^{-1}

point corresponds to the minimum value on the $-(d\theta/d\sigma)$ versus σ curve [15]. The corresponding $-(d\theta/d\sigma)$ versus σ plots for the Cu-Cr-Zr-Y alloy deformed at the 0.001 s^{-1} strain rate and varying temperature are shown in Fig. 3. It can be seen that all the curves have clear inflection points in Fig. 3(a) and the critical stress in Fig. 3(b). This indicates that DRX occurred at high temperatures and low strain rates. The critical stress related to the onset of DRX increases with decreasing temperature. This is because DRX is a thermally activated process, which cannot accumulate enough energy for the nucleation and growth of the DRX grains at lower temperature. Due to the increased severity of dislocation pileup, accumulated stress cannot be easily relaxed at low temperature. Thus, higher strain hardening rates and stress levels can be reached at lower deformation temperature. The higher the deformation temperature, the faster is the DRX kinetics. Similar effects were observed by Zhang et al. [16] in the Cu-Al alloys and by Ji et al. [17] in the Cu-Mg alloys.

3.4 Microstructure Evolution

Optical images of the Cu-Cr-Zr-Y alloy microstructure deformed at strain rate of 0.001 s^{-1} and different temperatures are shown in Fig. 4. It can be seen that the original grains were elongated along the deformation direction in Fig. 4(a). There are no obvious recrystallized grains observed except the occasional deformation bands. The main softening mechanism is dynamic recovery [18, 19]. With increasing the deformation temperature, the initial grain boundaries transformed to normal high-angle grain boundaries marked by arrows in Fig. 4(b). At the same time, some new DRX grains nucleated at the high-angle grain boundaries in Fig. 4(b) and (c). This demonstrates that the dynamic recrystallization occurred. According to Fig. 4(b) and (c), there is a large amount of refined recrystallized grains, which is much smaller than the starting grains observed. However, some elongated grains are still present in the deformed microstructure. This means that the dynamic recrystallization was not completed. When the sample was deformed at 800 °C and 0.001 s^{-1}, the original grains are replaced by the new DRX grains, indicating that the almost full dynamic recrystallization process is complete, as seen in Fig. 4(d). Finally, when the deformation temperature reached

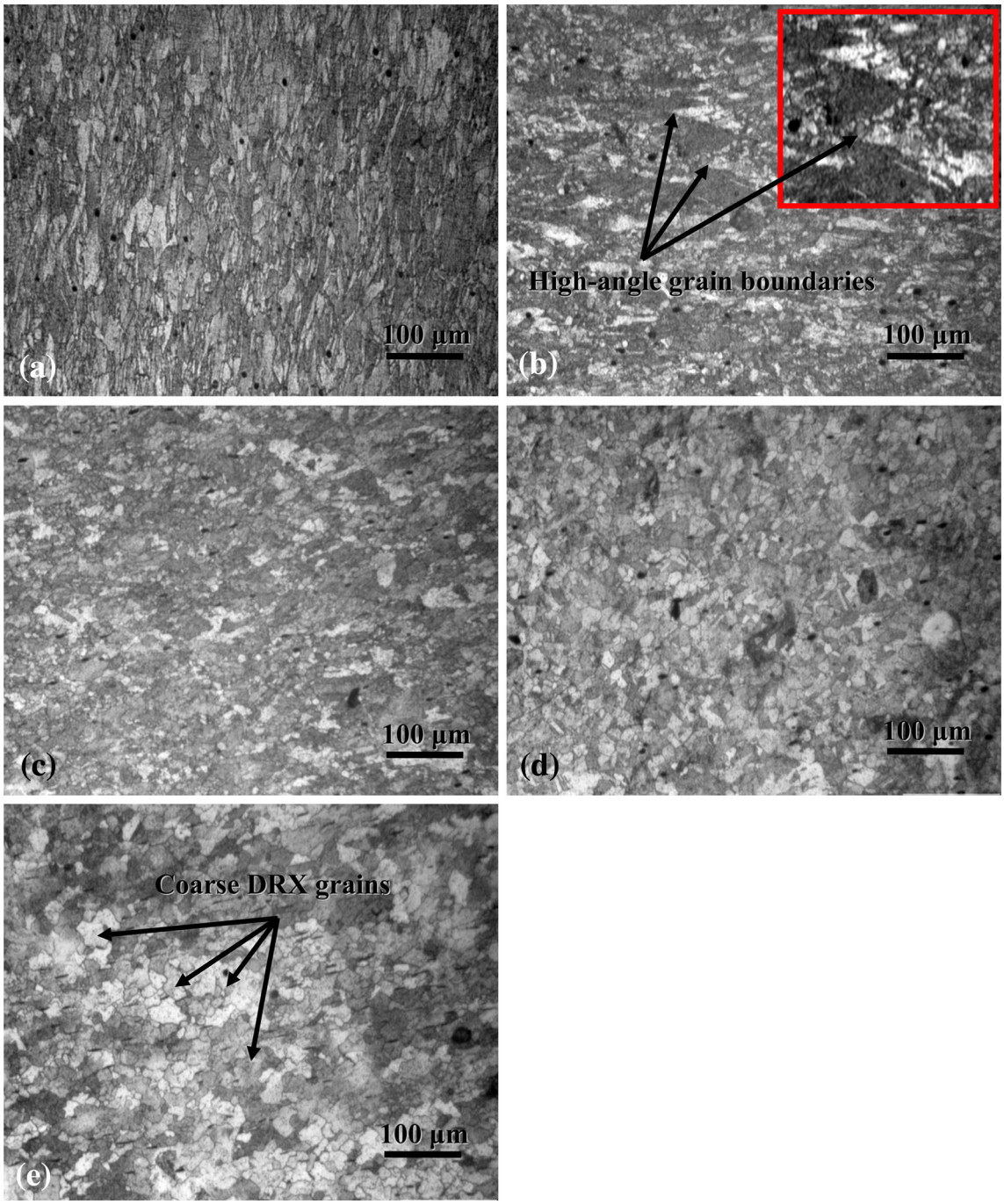

Fig. 4 Optical micrographs of the hot compressed specimen microstructure deformed at the strain rate of 0.001 s^{-1} and different temperatures: (a) 650 °C; (b) 700 °C; (c) 750 °C; (d) 800 °C; and (e) 850 °C

850 °C, the size of the DRX grains obviously increased and some coarsened DRX grains were observed. This indicates that the evolution of DRX microstructure strongly depends on the deformation conditions of temperature and strain rate. Dynamic recrystallization appears at high temperatures and low strain rates.

Zhang et al. [6] found that the addition of Ce can improve DRX of the Cu-Cr-Zr alloy during hot deformation. In this paper, the addition of Y also has important effects on the Cu-Cr-Zr alloy DRX. Figs. 5(a) and (b) show the microstructure of the Cu-Cr-Zr and Cu-Cr-Zr-Ce alloys after solution treatment, where Y addition can evidently refine the grain.

The microstructure of the Cu-Cr-Zr alloy deformed at 750 °C with the strain rate of 0.1 s^{-1} is shown in Fig. 6(a). It can be seen that some DRX grains were nucleated at the initial grain boundaries and deformation bands. Research results show that some low stacking fault energy materials, such as nickel base superalloy and austenitic stainless steel, have a typical "necklace-type" structure deformed at lower temperatures in hot working [20, 21]. This structure is the main mechanism of

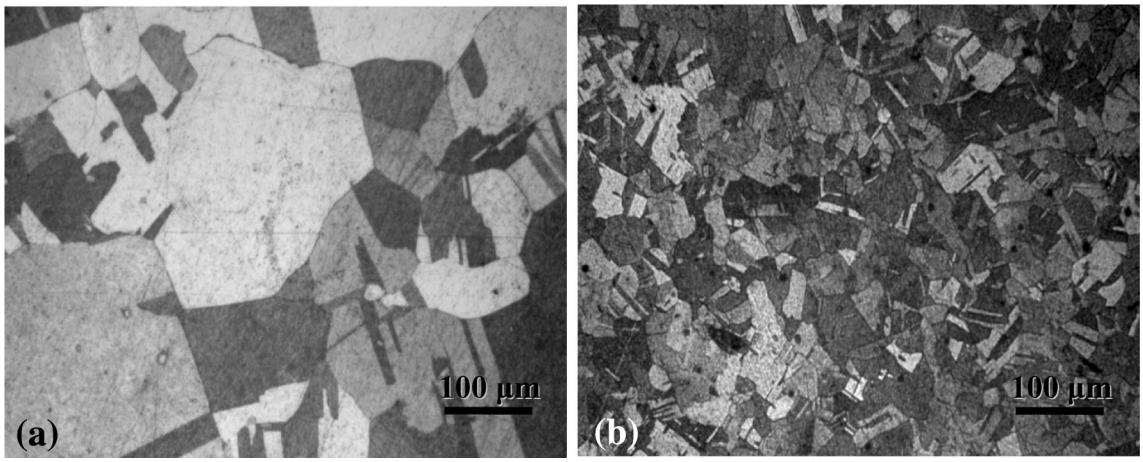

Fig. 5 Microstructure of (a) Cu-Cr-Zr and (b) Cu-Cr-Zr-Y alloys after solution treatment at 900 °C for 1 h

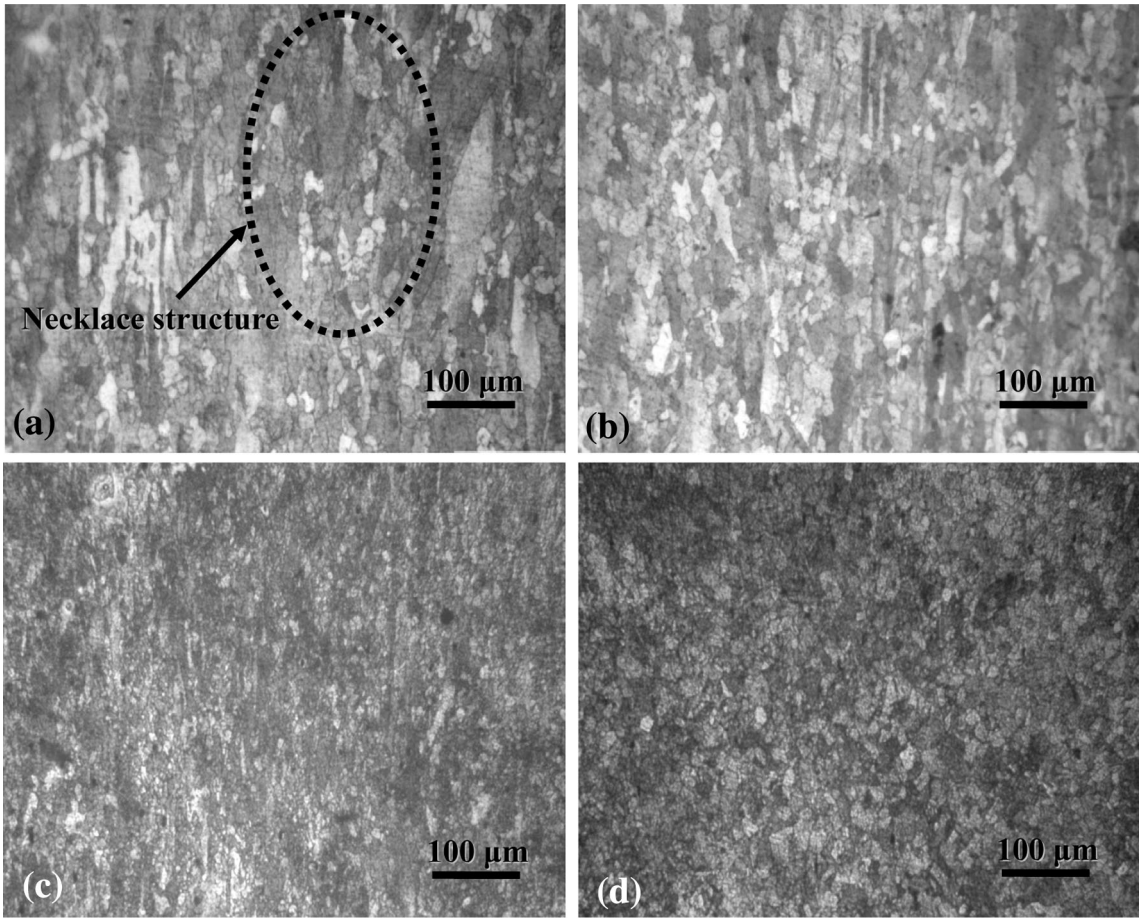

Fig. 6 Microstructure of (a-b) Cu-Cr-Zr and (c-d) Cu-Cr-Zr-Y alloys hot deformed at different conditions: (a) 750 °C and 0.1 s^{-1}; (b) 850 °C and 0.1 s^{-1}; (c) 750 °C and 0.1 s^{-1}; (d) 850 °C and 0.1 s^{-1}

recrystallization nucleation [22]. This is also observed in this study [marked by arrows in Fig. 6(a)]. Many more DRX grains along with a few elongated initial grains were observed when the temperature increased to 850 °C, as seen in Fig. 6(b), which also indicates that the DRX is not complete. Compared with the Cu-Cr-Zr-Y alloy deformed at the same conditions, the shear bands have become unclear, and a large number of smaller and uniform DRX grains were found in Fig. 6(c). A number of equiaxial DRX grains are seen in Fig. 6(d), where full DRX was obtained. This indicates that the addition of Y can refine the grain and improve dynamic recrystallization. The reason for this is that the DRX nucleation is improved by the increase of boundary areas, refined by the Y addition. These fine recrystallized grains can promote boundary movement and grain

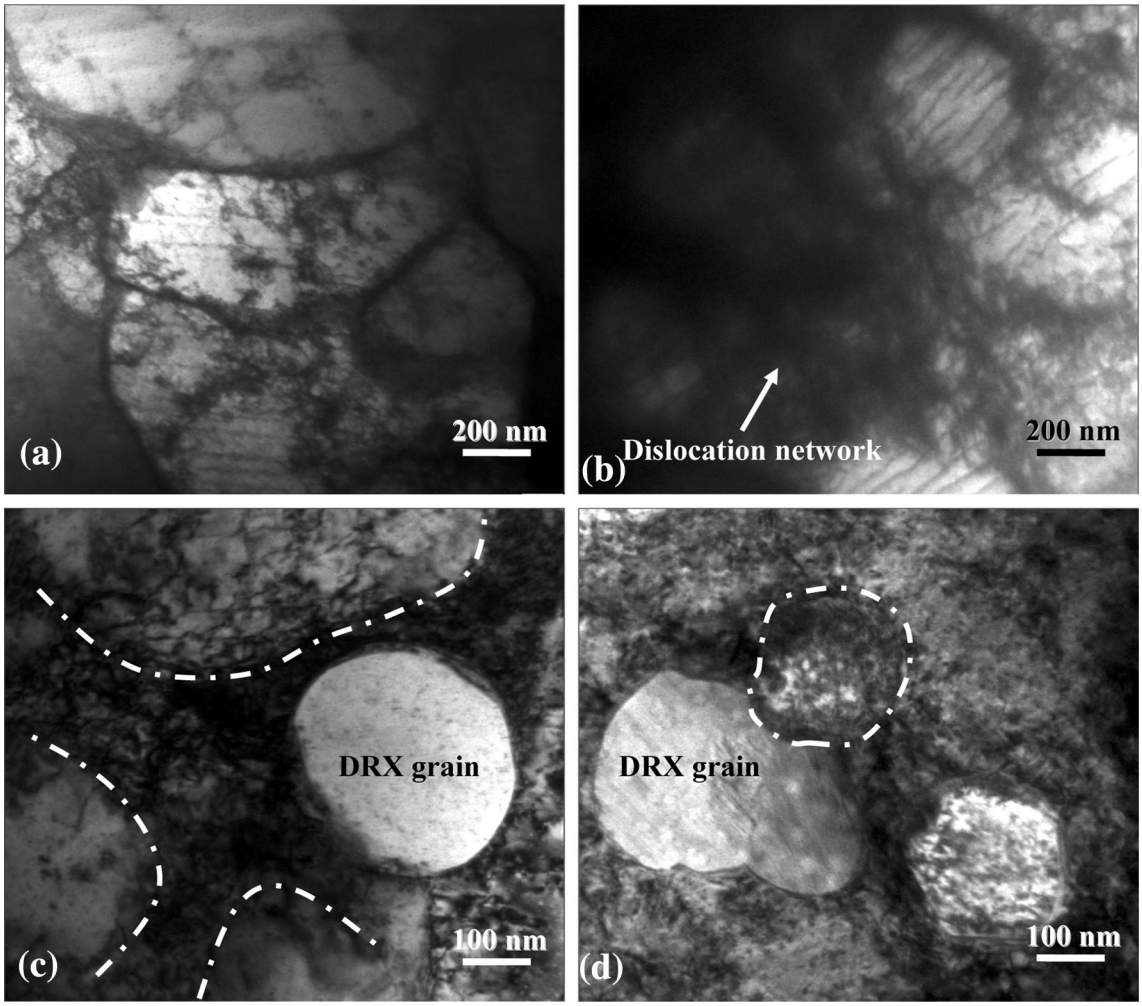

Fig. 7 TEM micrographs of the Cu-Cr-Zr-Y alloy deformed at different deformation temperatures and strain rates: (a) 700 °C and 0.1 s^{-1}; (b) 700 °C and 0.001 s^{-1}; (c) 800 °C and 0.001 s^{-1}; (d) 850 °C and 0.001 s^{-1}

rotation during the hot deformation [23]. During hot deformation many dislocations pile up and the addition of Y can increase accumulated energy and dislocation density. Therefore, the existence of accumulated energy and dislocations improves the driving force of recrystallized nucleation.

Fig. 7 shows TEM micrographs of the Cu-Cr-Zr-Y alloy deformed at the strain rates of 0.1 and 0.001 s^{-1} at 700, 800, and 850 °C, respectively. The grains are elongated in Fig. 7(a). Figure 7(b) shows that the dislocations are tangled and stored in the grain interior of the Cu-Cr-Zr-Y alloy deformed at 700 °C with the 0.001 s^{-1} strain rate. The dislocation climb and cross-slip in low stacking fault energy alloys are difficult at low deformation temperature. Thus, the high density dislocations are intersected and tangled, forming the network structure, which makes dislocation slip more difficult [24]. Due to the dislocation strengthening, the flow stress and strain hardening rate increase with the decrease of the deformation temperature. The rapid increase of the number of dislocations easily induces dynamic recrystallization once the dislocation density exceeds a critical value. Fig. 7(c) shows typical microstructure of the Cu-Cr-Zr-Y alloy, indicating the DRX occurrence. Fig. 7(c) indicates that the dislocation density is much lower compared with Fig. 7(b). The dislocations are piled up in the vicinity of grain boundaries. The dynamically recrystallized grains appear at the grain boundaries with dislocation tangles. The dislocation movement is a thermally activated process. High deformation temperature and low strain rate can provide sufficient energy for dislocation movement. Therefore, the nucleation of dynamically recrystallized grains appears at the high-angle grain boundaries marked by dashed lines in Fig. 7(c). The dislocation movement is enhanced with the deformation temperature increase, which can promote dynamic recrystallization. It can be seen that the dislocation density is greatly decreased in Fig. 7(d) compared with Fig. 7(c). The activation of dislocation movement accelerates the dislocation annihilation rate when the alloy is deformed at higher temperature. Once the critical strain is exceeded, dynamic recrystallization takes place and dynamic softening occurs [25–27]. When the deformation temperature is increased from 800 to 850 °C, some new dynamically recrystallized grains, marked by dashed line, can be found in Fig. 7(d).

4. Conclusions

It can be concluded that the dislocation generation and multiplication are the main hot deformation mechanisms for the

Cu-Cr-Zr-Y alloy. The increase of deformation temperature and the decrease of the strain rate can promote dynamic recrystallization of the alloy. In summary, the critical conditions for DRX were determined using the strain hardening rate. The deformation temperature and strain rate can strongly affect the deformed microstructure. Dynamic recrystallization appears at high temperature and low strain rate. The addition of Y can improve the dynamic recrystallization of Cu-Cr-Zr. Dislocation generation and multiplication are the main hot deformation mechanisms in this study. This information can be used for optimizing hot deformation processing parameters of the Cu-Cr-Zr-Y alloy.

Acknowledgments

This work was supported by the National Natural Science Foundation of China (51101052) and the by National Science Foundation (IRES 1358088).

References

1. J.H. Su, Q.M. Dong, P. Liu, H.J. Li, and B.X. Kang, Research on Aging Precipitation in a Cu-Cr-Zr-Mg Alloy, *Mater. Sci. Eng. A*, 2005, **392**, p 422–426
2. C.D. Xia, Y.L. Jia, W. Zhang, K. Zhang, Q.Y. Dong, G.Y. Xu, and M. Wang, Study of Deformation and Aging Behaviors of a Hot Rolled-Quenched Cu-Cr-Zr-Mg-Si Alloy During Thermomechanical Treatments, *Mater. Des.*, 2012, **39**, p 404–409
3. S.G. Mu, F.A. Guo, Y.Q. Tang, X.M. Cao, and M.T. Tang, Study on Microstructure and Properties of Aged Cu-Cr-Zr-Mg-RE Alloy, *Mater. Sci. Eng. A*, 2008, **475**, p 235–240
4. Z.Y. Ding, S.G. Jia, P.F. Zhao, M. Deng, and K.X. Song, Hot Deformation Behavior of Cu-0.6Cr-0.03Zr Alloy During Compression at Elevated Temperatures, *Mater. Sci. Eng. A*, 2013, **570**, p 87–91
5. G.L. Ji, Q. Li, K.Y. Ding, L. Yang, and L. Li, A Physically-Based Constitutive Model for High Temperature Deformation of Cu-0.36Cr-0.03Zr Alloy, *J. Alloys Compd.*, 2015, **648**, p 397–407
6. Y. Zhang, A.A. Volinsky, H.T. Tran, Z. Chai, P. Liu, and B.H. Tian, Effects of Ce Addition on High Temperature Deformation Behavior of Cu-Cr-Zr Alloys, *J. Mater. Eng. Perform.*, 2015, **24**, p 3783–3788
7. M.H. Wang, Y.F. Li, W.H. Wang, and J. Zhou, Quantitative Analysis of Work Hardening and Dynamic Softening Behavior of Low Carbon Alloy Steel Based on the Flow Stress, *Mater. Des.*, 2013, **45**, p 384–392
8. D.J. Li, Y.R. Feng, S.Y. Song, Q. Liu, and Q. Bai, Influences of Silicon on the Work Hardening Behavior and Hot Deformation Behavior of Fe-25wt%Mn-(Si, Al) TWIP Steel, *J. Alloys Compd.*, 2015, **618**, p 768–775
9. A. Etaati, K. Dehghani, G.R. Ebrahimi, and H. Wang, Predicting the Flow Stress Behavior of Ni-42.5Ti-3Cu During Hot Deformation Using Constitutive Equations, *Met. Mater. Int.*, 2013, **19**, p 5–9
10. D.G. Cram, H.S. Zuro, Y.J.M. Brechet, and C.R. Hutchinson, Modelling Discontinuous Dynamic Recrystallization Using a Physically Based Model for Nucleation, *Acta Mater.*, 2009, **57**, p 5218–5228
11. S.M. Abbasi and A. Shokuhfar, Prediction of Hot Deformation Behaviour of 10Cr-10Ni-5Mo-2Cu Steel, *Mater. Lett.*, 2007, **61**, p 2523–2526
12. G. Gottstein, M. Frommert, and M. Goerdeler, Prediction of the Critical Conditions for Dynamic Recrystallization in the Austenitic Steel 800H, *Mater. Sci. Eng. A*, 2004, **387**, p 604–608
13. H. Mirzadeh and M.H. Parsa, Hot Deformation and Dynamic Recrystallization of NiTi Intermetallic Compound, *J. Alloys Compd.*, 2014, **614**, p 56–59
14. A. Najafizadeh and J.J. Jonas, Predicting the Critical Stress for Initiation of Dynamic Recrystallization, *ISJJ Int.*, 2006, **46**, p 1679–1684
15. H.Y. Wu, J.C. Yang, J.H. Liao, and F.J. Zhu, Dynamic Behavior of Extruded AZ61 Mg Alloy During Hot Compression, *Mater. Sci. Eng. A*, 2012, **535**, p 68–75
16. Y. Zhang, N.R. Tao, and K. Lu, Effect of Stacking-Fault Energy on Deformation Twin Thickness in Cu-Al Alloys, *Scr. Mater.*, 2009, **60**, p 211–213
17. G. Ji, Q. Li, and L. Li, The Kinetics of Dynamic Recrystallization of Cu-0.4 Mg Alloy, *Mater. Sci. Eng. A*, 2013, **586**, p 197–203
18. Y. Han, H. Wu, W. Zhang, D.N. Zou, G.W. Liu, and G.J. Qiao, Constitutive Equation and Dynamic Recrystallization Behavior of As-cast 254SMO Super-Austenitic Stainless Steel, *Mater. Des.*, 2013, **69**, p 230–240
19. S.L. Semiatin, D.S. Weave, R.C. Kram, P.N. Fagin, M.G. Glavicic, R.L. Goetz, N.D. Frey, and M.M. Antony, *Metal. Mater. Trans. A*, 2004, **35A**, p 679–693
20. J. Wang, J. Dong, M. Zhang, and X. Xie, Hot Working Characteristics of Nickel-Base Superalloy 740H During Compression, *Mater. Sci. Eng. A*, 2013, **566**, p 61–70
21. D. Samantaray, S. Mandal, M. Jayalakshmi, C. Athreya, A. Bhaduri, and V.S. Sarma, New Insights into the Relationship Between Dynamic Softening Phenomena and Efficiency of Hot Working Domains of a Nitrogen Enhanced 316L(N) Stainless Steel, *Mater. Sci. Eng. A*, 2014, **598**, p 368–375
22. A. Momeni, S. Abbasi, M. Morakabati, H. Badri, and X. Wang, Dynamic Recrystallization Behavior and Constitutive Analysis of Incoloy 901 Under Hot Working Condition, *Mater. Sci. Eng. A*, 2014, **615**, p 51–60
23. Y.Y. Chen, B.H. Li, and F.T. Kong, Effects of Minor Yttrium Addition on Hot Deformability of Lamellar Ti-45Al-5Nb Alloy, *Trans. Nonferr. Metal. Soc.*, 2007, **17**, p 58–63
24. D.X. Wen, Y.C. Lin, J. Chen, X.M. Chen, J.L. Zhang, Y.J. Liang, and L.T. Li, Work-Hardening Behaviors of Typical Solution-Treated and Aged Ni-Based Superalloys During Hot Deformation, *J. Alloys Compd.*, 2015, **618**, p 372–379
25. N. Zhou, D.C. Lv, H.L. Zhang, D. McAllister, F. Zhang, M.J. Mills, and Y. Wang, Computer Simulation of Phase Transformation and Plastic Deformation in IN718 Superalloy: Microstructural Evolution During Precipitation, *Acta Mater.*, 2013, **65**, p 270–276
26. T.D. Kil, J.M. Lee, and Y.H. Moon, Quantitative Formability Estimation of Ring Rolling Process by Using Deformation Processing Map, *J. Mater. Process. Technol.*, 2015, **220**, p 224–230
27. H. Mirzadeh, Constitutive Description of 7075 Aluminum Alloy During Hot Deformation by Apparent and Physically-Based Approaches, *J. Mater. Eng. Perform.*, 2015, **24**, p 1095–1099